The Journal of Neuroscience, August 1987, 7(8): 2397–2411

Axonal Transport of Cytoskeletal Proteins in Oculomotor Axons and Their Residence Times in the Axon Terminals

Paola Paggi[1] and Raymond J. Lasek[2]

[1]Bio-architectonics Center, School of Medicine, Case Western Reserve University, Cleveland, Ohio 44106, and
[2]Department of Cellular and Developmental Biology, University "La Sapienza," 00185 Rome, Italy

Cytoskeletal protein transport and metabolism are studied in the somatic motor and parasympathetic axons of the chicken oculomotor system. Kinetic analyses of pulse-labeled proteins indicate that the neurofilaments are transported 2–3 times more rapidly in the somatic motor axons than in the parasympathetic axons. By contrast, the transport rates of the slow component b (SCb) proteins are very similar in these axons. The parasympathetic axons terminate in the ciliary ganglion, and radiolabeling curves from the ciliary ganglion can be used to study the kinetics of cytoskeletal protein removal from the terminals. The rate of removal directly determines the residence time of the cytoskeletal proteins in the ciliary ganglion, and the residence time directly affects the shape and amplitude of the transport curves of the ganglion. A computer model was used to analyze these transport curves and to determine the half-residence time of the cytoskeletal proteins in the terminal regions. From the computer experiments, we estimate that the half-residence times of the neurofilament proteins actin and tubulin are 2, 3.5, and 7 d, respectively. The differences between the half-residence times of the cytoskeletal proteins indicate that the rate of protein removal from the terminals differs for these proteins. On the basis of these results, we propose that the removal mechanisms critically control the composition of the cytoskeleton in the terminal regions. Through their effects on its composition, the removal mechanisms have a crucial role in converting the cytoskeleton of the axon proper into the specialized cytoskeleton of the axon terminal.

The cytoskeleton of the axon is a dynamic system. The proteins that constitute the axonal cytoskeleton are produced by the synthetic machinery in the nerve cell body and they are actively conveyed in the axon by the mechanisms of slow axonal transport (Lasek et al., 1984). Pulse-labeling experiments indicate that the cytoskeletal proteins are metabolically stable during their passage through the axon, and, essentially, all of these proteins complete the trip to the axon terminal (Hoffman and Lasek, 1975; Lasek and Black, 1977).

Received Sept. 29, 1986; revised Jan. 5, 1987; accepted Jan. 30, 1987.

This research was supported by the National Institutes of Health (R.J.L.); travel expenses for P.P. were supported by CNR Grant 85,00659,04 and MPI Grant 1985. Shirley Ricketts and Diane Filsinger provided excellent technical assistance, and Dr. Michael J. Katz assisted with the exposition of both the algorithm and the computer-modeling experiments.

Correspondence should be addressed to Dr. Raymond J. Lasek at the above address.

On the basis of these observations and others, Lasek and Hoffman (1976) proposed that, after the cytoskeletal proteins are transported into the axon terminals, they are degraded by the proteases operating locally in the terminal and eliminated from the axon. In this model of cytoskeletal protein metabolism, proteases are present throughout the axon (Schlaepfer and Micko, 1979; Pant and Gainer, 1980; Kamakura et al., 1983; Malik et al., 1984; Schlaepfer and Zimmerman, 1985). Nonetheless, they actively degrade the cytoskeleton proteins only in the axon terminal. The model is supported by the observation that a protease inhibitor, leupeptin, blocks the removal of neurofilaments from the axon terminal of goldfish retinal ganglion cells (Roots, 1983).

Kinetic studies of pulse-labeled proteins indicate that some cytoskeletal proteins, such as the neurofilament proteins, are degraded rapidly after they enter the terminal, whereas others, such as actin, reside in the terminal for days before they are degraded (Lasek and Black, 1977). Through their differential effects on the residence times of the cytoskeletal proteins in the terminal, the removal mechanisms control the composition of the cytoskeleton in the axon terminal (Lasek and Katz, 1987) and, because the cytoskeleton provides the framework for nerve terminal architecture, the removal mechanisms critically determine the internal structure and shape of nerve terminals.

To study cytoskeletal protein metabolism in axons requires an experimental model system that allows ready access to both the axons and their terminals. The chicken oculomotor system effectively fulfills these requirements (Droz et al., 1973; Filliatreau and Di Giamberardino, 1982). It consists of 2 separate and parallel populations of axons—the parasympathetic preganglionic axons and the somatic oculomotor axons. The somatic motor and parasympathetic axons originate from neurons in the same nucleus and can be labeled simultaneously with a single injection of labeled amino acids. These axons exit the midbrain together, forming the oculomotor nerve; they are then completely separated in the preganglionic and somatic divisions of the nerve (Fig. 1).

All of the parasympathetic preganglionic axons terminate in the ciliary ganglion 11 mm from the oculomotor nucleus (Fig. 1), and all of the somatic motor axons continue uninterrupted through the somatic oculomotor nerve branches (M1 and M2). Segments from both the somatic oculomotor nerve branch and the ciliary ganglion can be sampled 11 mm from the oculomotor nucleus (segments M1 and G, Fig. 1). Thus, the geometry of the system permits the direct comparison of the transport kinetics in the somatic motor axons with those in the parasympathetic axon terminals at the same distance from the oculomotor nucleus.

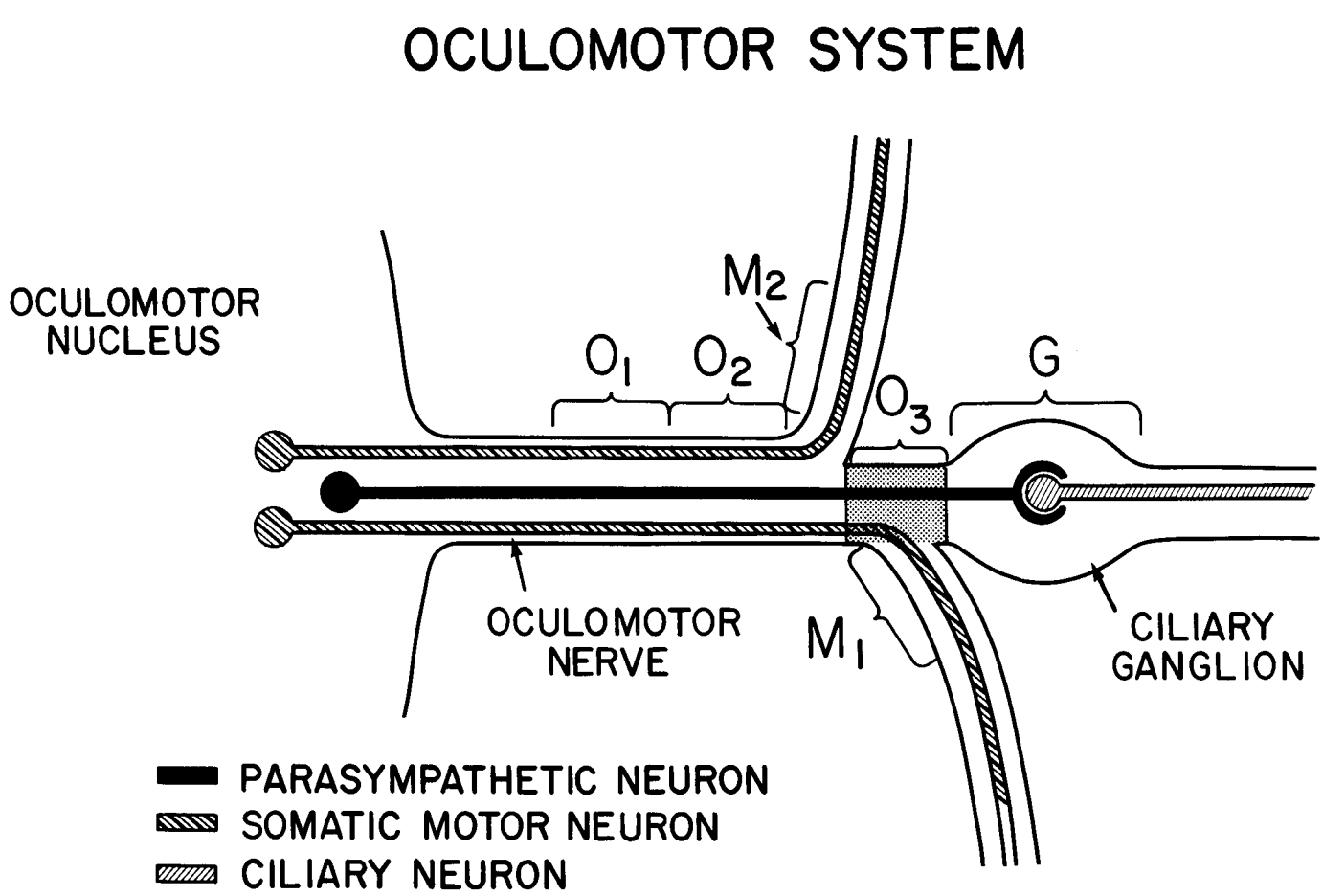

Figure 1. A schematic representation of the chicken oculomotor system showing the distribution of the somatic motor and parasympathetic axons. The axons originate in the oculomotor nucleus and traverse the oculomotor nerve together. They separate into the dorsal (*M2*) and ventral (*M1*) somatic motor branches of the oculomotor nerve and the ciliary ganglion (*G*). M1 and M2 contain only somatic motor axons and the ciliary ganglion contains the parasympathetic axons and their terminals. Segments *O1, O2, O3,* and *M2* are located, respectively, 7, 8.5. 9.5, and 9.5 mm from the oculomotor nucleus. Segments M1 and G are both located 11 mm from the nucleus.

We analyze here the passage of pulse-labeled cytoskeletal proteins through the chicken oculomotor system. Specifically, the transport rates in the somatic motor and parasympathetic axons are compared and the residence times of the cytoskeletal proteins in the axon terminals of the ciliary ganglion are determined.

Materials and Methods

Injection and radiolabeling of axonally transported proteins. Three-week-old Leghorn chickens were anesthetized with methoxyfluorane (Metofane, Pitman, Moore), and 500 μCi of 35 S methionine (sp act > 800 mCi/mM; New England Nuclear, Boston, MA) in 5 μl of 0.9% NaCl was injected through the skull into the cerebral aqueduct of each animal. The labeled amino acid reaches the oculomotor nucleus (located near the cerebral aqueduct), where the cell bodies of the preganglionic fibers (autonomic nucleus), as well as of the motor fibers (somatic nucleus) innervating the extrinsic eye muscles, are located (Fig. 1). Both the preganglionic and the motor axons course in the oculomotor nerve to the ciliary ganglion and to the extrinsic eye muscles, respectively.

Dissection and preparation of the tissue extracts. The chickens were decapitated at different time intervals, ranging from 18 hr to 93 d after injection. The ciliary ganglion, together with the related nerves (oculomotor system; Fig. 1), were dissected out, the tissue being kept in ice-cold 0.9% NaCl. As shown in Figure 1, the following segments were collected from the dissected oculomotor system: (1) 3 consecutive segments of the oculomotor nerve—O1, O2, and O3—1.5 mm each, containing both the somatic and preganglionic parasympathetic fibers; (2) 1.5 mm of the dorsal (M2) and ventral (M1) somatic oculomotor branches; and (3) the ciliary ganglion, which contains the terminals of the preganglionic fibers. The dissected segments O1, O2, O3, M1, M2, and G are respectively located 7, 8.5, 9.5, 11, 9.5, and 11 mm from the injected cell bodies.

The homologous segments removed from the left and right side of each chicken were combined and homogenized in 100 μl BUST (0.1 M Tris containing 2% beta-mercaptoethanol, 8 M urea, 1% SDS, pH 6.8) with a ground-glass microhomogenizer. The homogenate was then centrifuged at 22,000 × *g* (Sorvall SS-34 rotor) for 20 min at room temperature. An aliquot (5 μl) of each supernatant was used to determine total radioactivity (data were corrected for quenching by external standardization). Only a negligible amount of trichloroacetic acid (TCA)-soluble radioactivity was present in the samples 1 d or more after labeling (Filliatreau and Di Giamberardino, 1982, and unpublished observations). A measured aliquot (35–45 μl) from the remaining sample was analyzed by 1- and 2-dimensional SDS–PAGE.

SDS–PAGE and fluorography. Gradient slab gels (6–17.5% acrylamide) with a 4% stacking gel were used according to the procedure of Laemmli (1970). Two-dimensional isoelectrofocusing/SDS–PAGE was performed according to O'Farrel (1975), employing the standard range of ampholines (pH 5–7; LKB Instruments). The molecular-weight standards used were (in kDa): myosin (200), phosphorylase A (94), bovine serum albumin (68), pyruvate kinase (57), ovalbumin (43), carbonic anydrase (30), and lysozyme (14). Gels were stained with 1% Coomassie blue in 7% acetic acid and 35% methanol; destaining was performed with mild agitation in a solution of 35% methanol and 7% acetic acid.

The radioactive polypeptides were visualized by fluorography according to the method of Bonner and Laskey (1974) and Laskey and Mills (1975). Gels were prepared for fluorography by dehydration in dimethyl sulfoxide, impregnation with 2,5-diphenyloxazole (New England Nuclear), rehydration and vacuum drying into dialysis membrane.

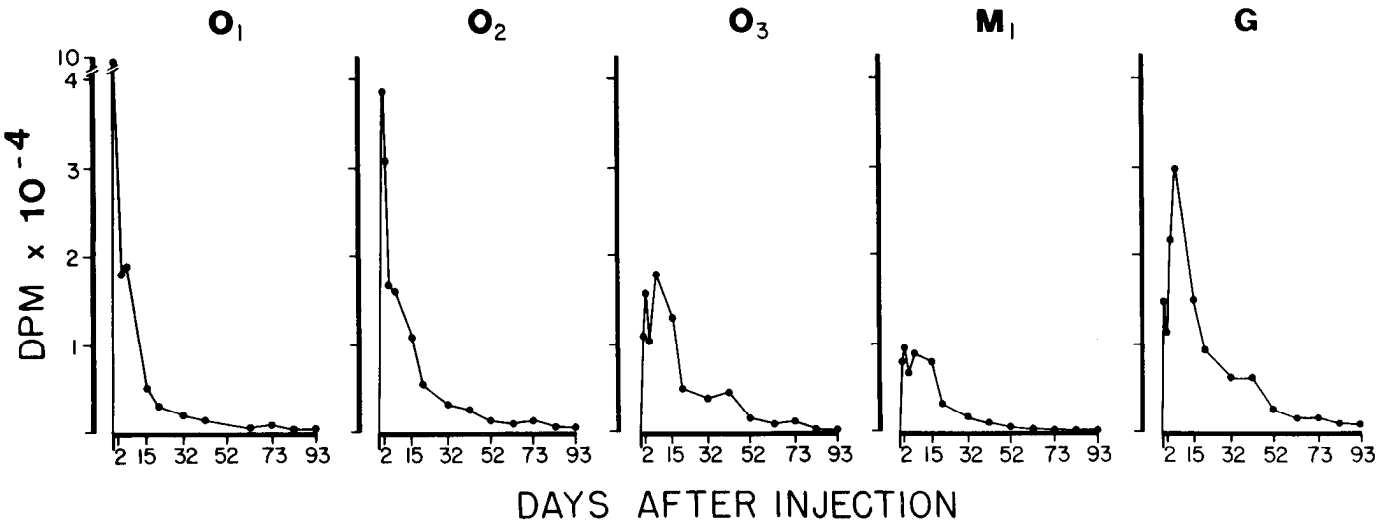

Figure 2. Axonal transport kinetics of radiolabeled, slowly transported proteins in segments of the oculomotor system obtained 1, 2, 4, 7, 15, 20, 32, 42, 52, 73, 83, and 93 d after labeling the oculomotor nucleus neurons. The window method was used to observe the passage of the pulse-labeled wave through 1.5 mm segments of the oculomotor nerve (*O1, O2, O3*), the somatic motor ventral branch (*M1*), and the ciliary ganglion (*G*). *Points* are averages of data from 3 to 8 animals; the data from 65 animals are represented.

Fluorographs were made using XR-5 x-ray film (Kodak) and incubation was at −70°C.

Quantification of radioactivity in individual transported proteins. Appropriate regions of the 1-dimensional gels were excised, using the fluorographs to locate the position of the labeled polypeptides in the gel. Gel slices were then solubilized by incubation in 0.5 ml of 30% hydrogen peroxide for 48 hr at 60°C. Radioactivity was quantified by liquid scintillation counting (Beckman LS 335 counter) using Formula 963 (New England Nuclear) as scintillant. The efficiency of counting was 25–35% by internal standardization. Counts were corrected for quenching and converted to disintegration per minute (dpm).

For most of the proteins that were analyzed, 1-dimensional PAGE provided sufficient separation of the labeled proteins for accurate quantitation of individual proteins. Actin was the only exception to this rule. The 2-dimensional gels demonstrated that several labeled proteins overlap the actin band on 1-dimensional PAGE. This problem was solved by using 2-dimensional PAGE to determine how much radioactivity was present in each of the proteins at 43 kDa and then by using this information to estimate the amount of radiolabeled actin in the excised 43 kDa band on 1-dimensional PAGE.

Determination of the pulse-transient. The pulse-transient is a mathematical summary of the transport curve that was obtained as follows: The mean radioactivity associated with either the total proteins or individual polypeptides was plotted, and the area under the curve was integrated using a Vanguard motion analyzer (Vanguard Instrument Corp., Melville, NY). The inegrated area under the transport curve was equal to the pulse-transient.

Results

The window method of analyzing axonal transport in the oculomotor system

Figure 2 illustrates the axonal transport kinetics of radiolabeled proteins in the oculomotor system 1–93 d after labeling. The data for individual segments (O1, O2, O3, G, and M1) are plotted as a function of the interval between injecting the radioactive precursor and collecting the segments for analysis. This method treats each segment of nerve as a "window" through which the transported proteins can be viewed (Levine and Willard, 1980; Brady and Lasek, 1982). Pulse-labeled structures that move at different rates can be distinguished as separate waves of radioactivity that pass by each window.

Radiolabeling studies show that axonal transport consists of 3 major transport waves. The fast component has a rate of 250–400 mm/d; slow component b (SCb) has a rate of 2–8 mm/d; and slow component a (SCa) has a rate of 0.2–2 mm/d (Lasek and Brady, 1982). Because of these differences in transport rates, the waves separate as they move away from their starting position in the nerve cell bodies (Fig. 2). Thus, wave separation is greater in distal than in proximal segments (compare O1 and O3 in Fig. 2).

Rapidly transported proteins in the oculomotor system

Within a few hours after labeling, the fast component proteins pass through the oculomotor axons and reach the ciliary ganglion in segment G (Droz et al., 1973). SDS–PAGE analyses of the radiolabeled proteins demonstrate that all of the radioactivity in segment G at 18 hr postinjection is due to fast component proteins, and that between 18 hr and 2 d the amount of radiolabeled fast component proteins in segment G declined (Fig. 3). At 4 d, these proteins were almost completely removed from segment G (arrowheads in Fig. 3). These results support the proposal that the mean time of sojourn of the fast component proteins is 17 hr in chick parasympathetic axon terminals (Droz et al., 1973).

In contrast to segment G, segments O2 and M1 contained a very small amount of the radiolabeled fast component proteins (Figs. 3, 4). This finding indicates that only a small amount of the fast component proteins are deposited during their transit within the oculomotor axons; instead, most of these proteins are destined for the axon terminals (Bennett et al., 1973; Di Giamberardino et al., 1973; Droz et al., 1973).

Slow transport waves

Figure 2 shows that the waveform of segment M1 consists of 2 waves which peaked at 2 and 7 d. The waveform of segment G also consists of 2 waves which peaked at 7 and 42 d. Comparison of these waveforms with that of segment O3 indicates that the rates of slow transport differ between the somatic motor and parasympathetic axons. Segment O3 contains both the somatic motor and parasympathetic axons, and the waveform of segment O3 consists of 3 waves that peak at 2, 7, and 42 d. The

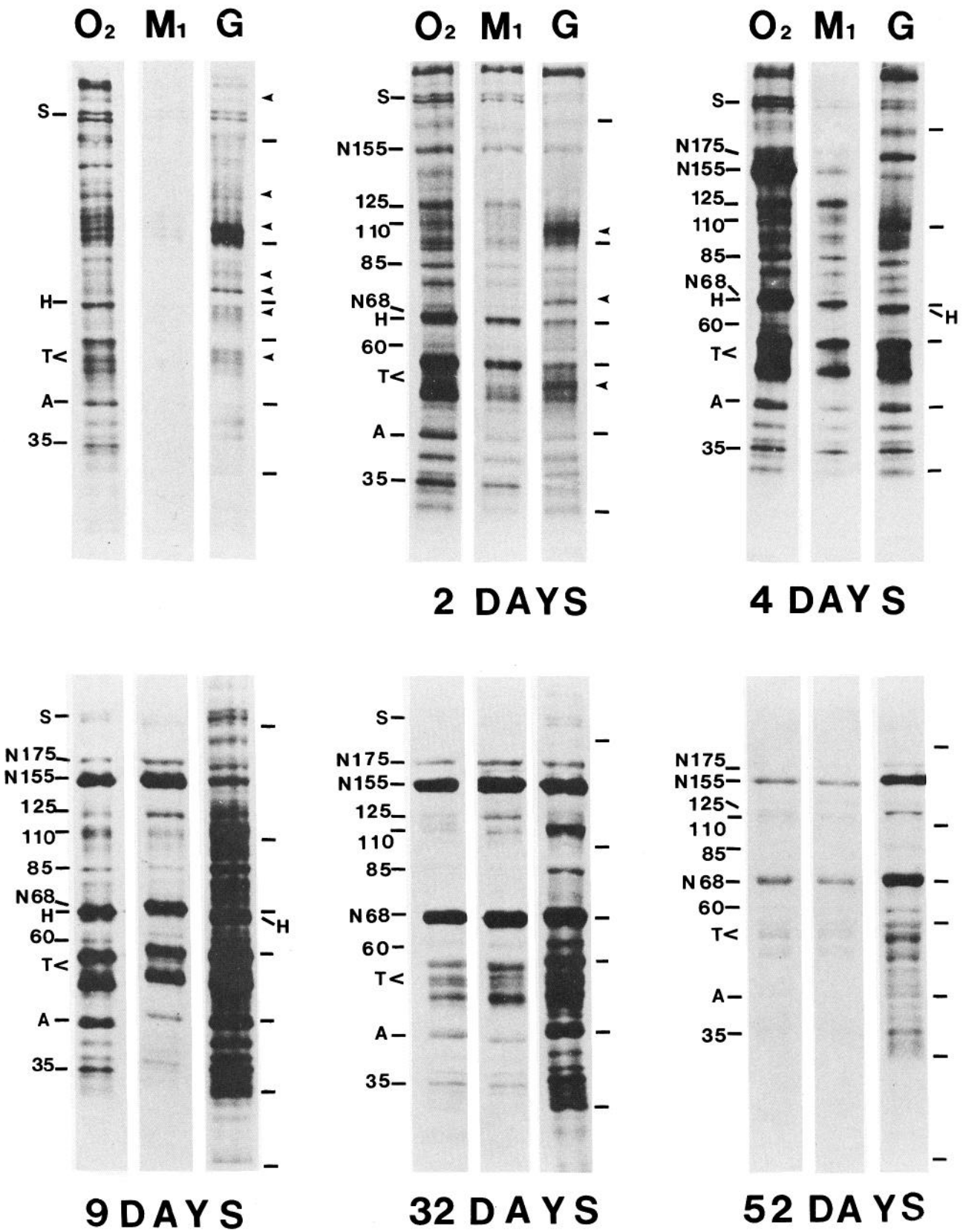

Figure 3. Fluorographs showing labeled polypeptides separated by 1-dimensional SDS–PAGE at 18 hr and 2, 4, 9, 32, and 52 d after labeling the oculomotor neurons. Aliquots of homogenates from nerve segments (see Materials and Methods) were analyzed on gradient slab gels (4–17.5% acrylamide). *Bars at the right* indicate the positions of the molecular-weight markers (200, 94, 68, 57, 43, 30, and 14 kDa, reading *top to bottom*). *Arrowheads at the right* indicate major polypeptides of the fast component of the axonal transport. The bands corresponding to major polypeptides of the slow component of the axonal transport are indicated by labels: brain spectrin (*S*), putative heat-shock proteins (*H*), the polypeptides at 125, 110, 85, 60, and 35 kDa, actin (*A*), tubulin (*T*) and the neurofilament proteins (*N175, N155, N68*).

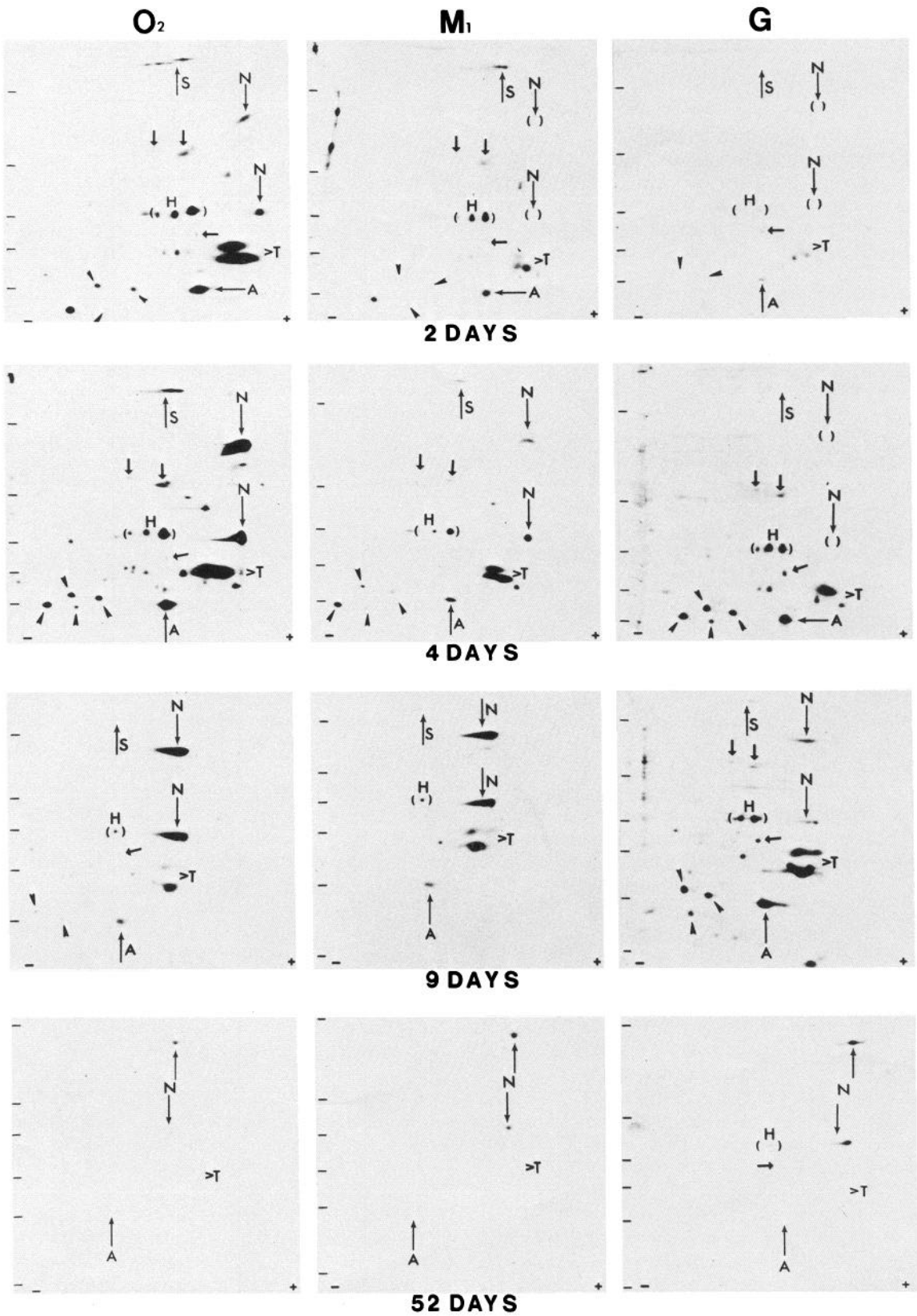

Figure 4. Fluorographs showing labeled polypeptides separated by 2-dimensional SDS–PAGE at 2, 4, 9, and 52 d after labeling the oculomotor nucleus neurons. Aliquots of segment homogenates (see Materials and Methods) were subjected to isoelectric focusing in the first dimension, then electrophoresed on 4–17.5% gradient slab polyacrylamide gels in the second dimension. Acidic and basic portions of the gels are indicated. *Bars at the left* indicate the positions of the molecular-weight markers (200, 94, 68, 57, 43, and 30 kDa, reading *top to bottom*). Major polypeptides of the slow component of the axonal transport are indicated by labels: brain spectrin (*S*), putative heat-shock proteins (*H*), the 43 kDa cluster (*arrowheads*), 125, 110, and 60 kDa (*arrows*), actin (*A*), tubulin (*T*), and neurofilament proteins (*N*).

peaks at 2 and 7 d in segment O3 correlate with the 2 peaks in the somatic motor axons (segment M1), and the peaks at 7 and 42 d in segment O3 correlate with the peaks in the parasympathetic axons (segment G).

These results suggest that the waveform of segment O3 is a composite of 4 waves—2 that peak at 2 and 7 d in the somatic motor axons and 2 that peak at 7 and 42 d in the parasympathetic axons. Because both the somatic motor and parasympathetic axons have a wave that peaks at 7 d, these waves overlap in segment O3 and only 3 of the 4 waves are resolved in this segment.

SDS–PAGE analyses of the slowly transported proteins

To more effectively compare the kinetics of the slowly transported proteins in the somatic motor and parasympathetic axons, the radiolabeled proteins were separated by SDS–PAGE and visualized by fluorography. Examination of more than 300 fluorographs made from preparations obtained between 18 hr and 93 d postinjection indicated that the data derived from segments O2, M1, and G at 18 hr and 2, 4, 9, 32, and 52 d after labeling represented the most significant aspects of slow transport through the oculomotor axons; these are illustrated in Figure 3. To further resolve the polypeptide patterns, the radiolabeled proteins were separated by 2-dimensional PAGE. Figure 4 shows representative 2-dimensional PAGE fluorographs from animals at 2, 4, 9, and 52 d postinjection. Detailed kinetics of slowly transported proteins were obtained by quantitative analysis of radiolabeled bands in the polyacrylamide gels (Figs. 5, 6).

Transport kinetics of individual slowly transported proteins

Cytoskeletal structures, such as microtubules, microfilaments, and neurofilaments, are the natural units of slow axonal transport (for a review, see Lasek and Brady, 1982; Lasek et al., 1984), and the transport kinetics of these structures can be studied by pulse-labeling their protein subunits. These pulse-labeling studies demonstrate that the slowly transported proteins can be classifed into 2 subcomponents of slow transport, SCa and SCb (Black and Lasek, 1980; Lasek et al., 1984). In the following section, we use the results from the one- and two-dimensional PAGE analyses to describe the kinetics of individual, slowly transported proteins with regard to their transport in SCa and SCb.

The 35 kDa protein and other SCb proteins. SCb consists of a diverse population of axonal proteins that can be identified by their transport rate and by analysis with two-dimensional PAGE (Tytell et al., 1981; Brady and Lasek, 1982; Garner and Lasek, 1982). At 18 hr postinjection, the SCb proteins were present in segment O2 but not in segments M1 or G (Figs. 3, 4). At 2 d, the SCb proteins had reached segments M1 and G, as shown clearly by two-dimensional PAGE (Fig. 4).

The fluorographs in Figures 3 and 4 indicate that the SCb proteins arrive in segment M1 before they arrive in segment G. For example, at 2 d postinjection, very little of the radiolabeled SCb proteins had reached segment G (Figs. 3, 4). In contrast, in segment M1 at 2 d postinjection, a number of the SCb proteins, including the heat-shock proteins, were major radiolabeled spots on the fluorographs (H in Figs. 3, 4). Because segments M1 and G are both located at the same distance (11 mm) from the injection site, the observation that the proteins appear earlier in segment M1 than in segment G suggests that the front of the SCb wave is transported slightly faster in the somatic motor axons than in the parasympathetic axons. The exact determination of this small difference will require more time points between 12 and 18 hr after injection.

The transport curves of individual SCb proteins of segment M1 differ from those of segment G (Fig. 5). In segment M1, the waveforms of the 35, 110, and 125 kDa proteins reached a peak at 2 d. By contrast, in segment G, the waveforms of these proteins reached a peak at 7 d. Moreover, the proteins were present in segment G much longer than in segment M1; specifically, the 35 kDa protein was almost completely removed from segment M1 at 20 d, and a substantial amount of the radiolabeled 35 kDa protein was present in segment G after 20 d. These results suggest that the SCb proteins reside longer in segment G than in segment M1.

Actin. Kinetic analyses of actin transport in axons demonstrate that actin is conveyed with the SCb wave (Black and Lasek, 1979; McQuarrie et al., 1986). In some neurons, a substantial amount of actin is also transported with SCa (Mori et al., 1979; McQuarrie et al., 1986; Oblinger et al., 1987). Likewise, in segment M1, the actin waveform has 2 subcomponents, one that corresponds to SCb and another that corresponds to SCa. The peak of the first wave of actin arrived in segment M1 at 2 d, coincident with the arrival of the 35 kDa protein and other SCb proteins (Fig. 5). The peak of the second actin wave arrived in segment M1 at 7 d. This slower-moving wave corresponds to SCa and traversed segment M1 with the neurofilament wave (Fig. 6).

In segment G, the SCb wave of actin reached a peak at 7 d, coincident with the 35 kDa protein peak (Fig. 6). However, the crest of the actin wave was not as sharp as that of the 35 kDa protein. A second, very slow wave of actin peaked at 42 d. This slowly moving wave of SCa actin coincides with the wave of neurofilament proteins in the parasympathetic axons (Fig. 6).

Tubulin. The fluorographs show that a small amount of radiolabeled tubulin first reached segments M1 and G with the front of the SCb proteins (Figs. 3, 4). This finding indicates that some tubulin is transported with SCb in both the somatic motor and parasympathetic axons. Tubulin also moves with SCb in mammalian ventral motor neurons (McQuarrie et al., 1986).

In segment M1, the tubulin transport curve has 2 distinct components, a small leading component that traversed M1 between 2 and 9 d, and a large wave that peaked at 7 d (Fig. 6). The small leading wave arrived in segment M1 at 2 d, at the same time as the front of the 35 kDa protein wave; it represented microtubules transported with SCb. The large, more slowly moving wave traversed segment M1 between 7 and 21 d, at the same time as the neurofilament protein wave; it represented the microtubules transported with SCa (Fig. 6). Although the overall distribution of the SCa tubulin wave was similar to that of the neurofilament wave, the tubulin wave peaked at 7 d and the neurofilament wave peaked at 15 d.

In segment G, the SCb tubulin formed a sharp peak at 7 d; this peak was coincident with the peak of the 35 kDa protein (Fig. 6). As with actin, the tubulin waveform had a trailing component between 20 and 52 d postinjection. This trailing component of SCa tubulin traversed segment G with the main wave of the neurofilaments (Fig. 6).

Neurofilament proteins. Kinetic studies of neurofilament transport in many different kinds of neurons demonstrate that these structures are normally transported with SCa (Lasek and Hoffman, 1976; Mori et al, 1979; Black and Lasek, 1980; McQuarrie et al., 1986). Likewise, in the oculomotor axons, the

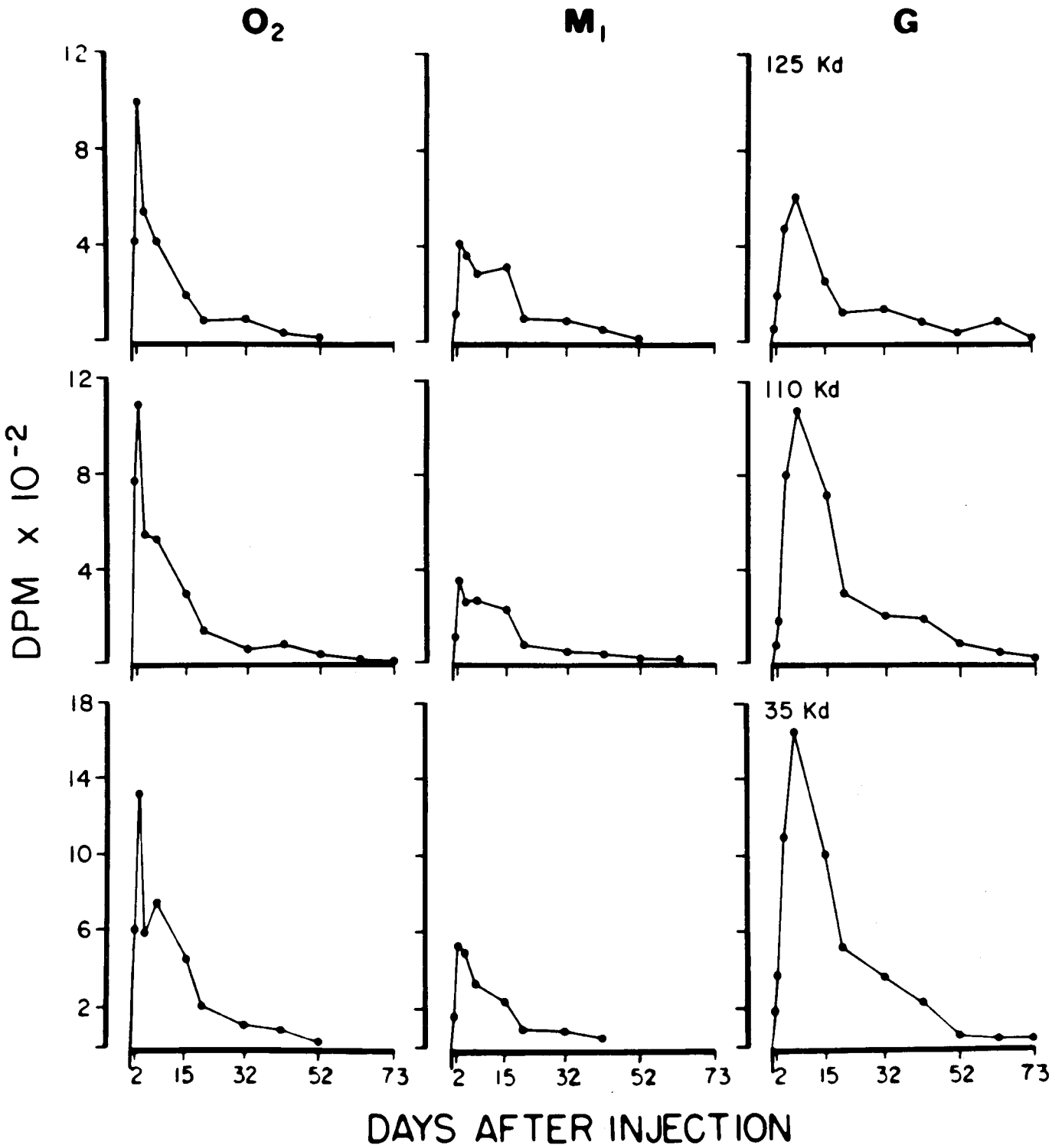

Figure 5. Quantitative analyses of the transport profiles of individual SCb proteins at 1, 2, 4, 7, 15, 20, 32, 42, 52, 73, 83, and 93 d after labeling the oculomotor nucleus neurons. Data from fluorographs like those in Figure 3 were used to remove the gel regions containing the 125, 110, and 35 kDa polypeptides. Data for 1.5 mm of oculomotor nerve segment (*O2*) and its somatic motor ventral branch (*M1*), and for the ganglion (*G*) are plotted as a function of the interval between injecting the radioactive precursor and collecting the segments for analysis. *Points* are averages of 2–7 observations for a total of 60 observations. In segment M1, the waveforms of the proteins reached a peak at 2 d. In segment G the waveforms of the proteins reached a peak at 7 d; the proteins were present in segment G much longer than in segment M1.

neurofilament proteins are transported as a separate wave that moves more slowly than the SCb wave.

The separation between the SCb and neurofilament proteins is illustrated most clearly by a comparison of the arrival of the SCb and neurofilament wave fronts. In segment M1, the fronts of the SCb wave and the neurofilament wave arrived at 2 and 4 d (Figs. 4–6). In segment G, the SCb and neurofilament wave fronts arrived at 4 and 9 d, respectively (compare the fluorographs at 4 and 9 d in Fig. 4).

In both segments M1 and G, the neurofilament proteins formed

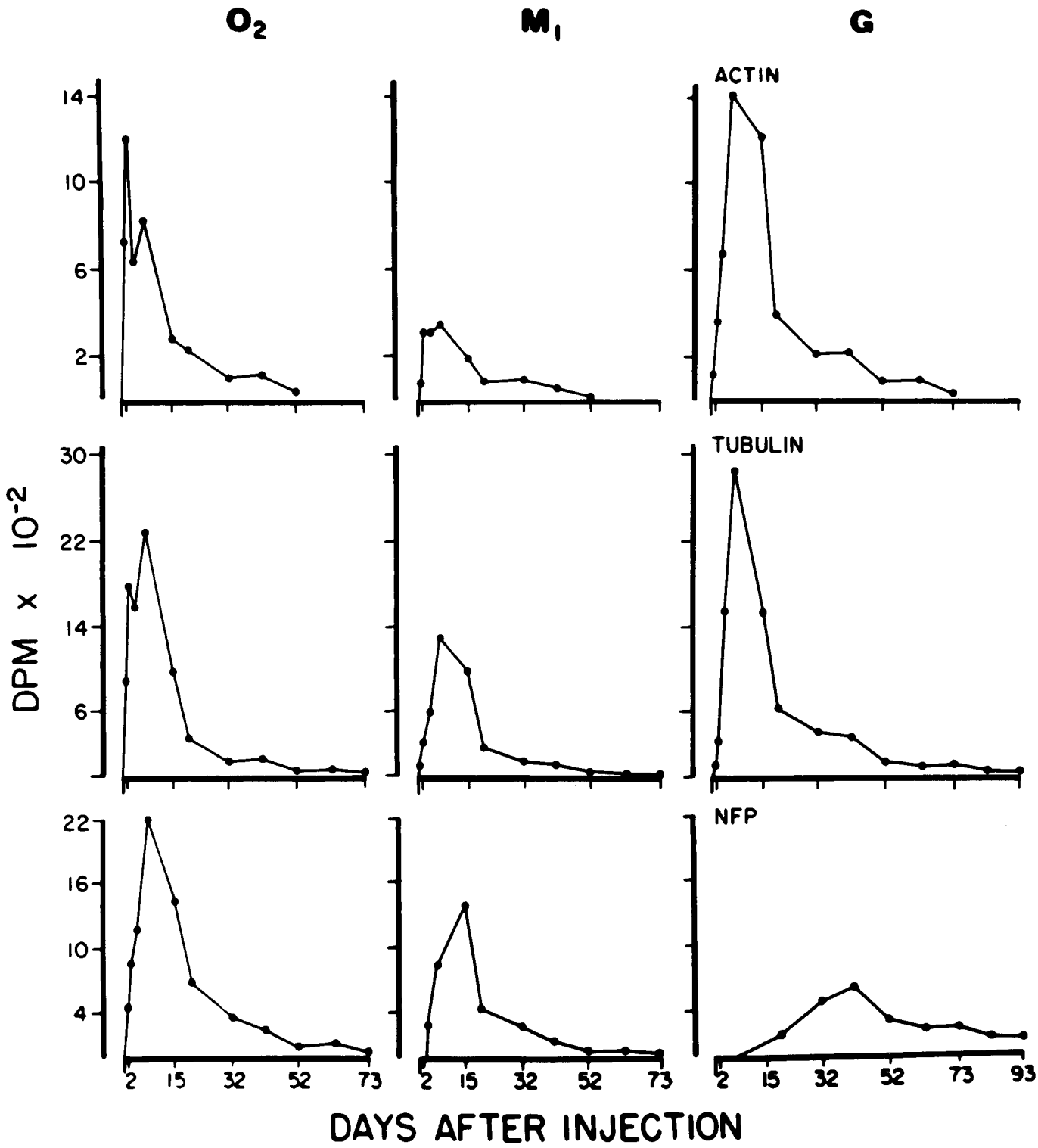

Figure 6. Axonal transport kinetics of radiolabeled cytoskeletal proteins. Data were obtained by punching spots from gels, as described in the legend to Figure 5 and in Materials and Methods. In segments *M1* and *G*, the waveform of actin shows 2 peaks at 2 and 7 d and at 7 and 42 d, respectively. In segment M1 the waveform of tubuiln shows a leading wave that crested between 2 and 4 d and a large wave that peaked at 7 d. In segment G the waveform of tubulin shows a peak at 7 d and a trailing component between 20 and 52 d. The waveforms of neurofilament proteins (*NFP*) show only one peak, both in M1 and G, at 15 d and 42 d, respectively.

a main peak that was followed by a trailing component (Fig. 6). In segment M1, the neurofilament peak arrived at 15 d; it arrived in segment G at 42 d (Fig. 6). The difference between the arrival times of the neurofilament waves in segments M1 and G suggests that the rate of neurofilament transport is more than 2 times faster in the somatic motor axons than in the parasympathetic axons (0.73 mm/d versus 0.26 mm/d, respectively). These results indicate that the somatic motor and parasympathetic axons

of the oculomotor nerve cannot be treated as a simple homogeneous system for studying axonal transport (Filliatreau and Di Giamberardino, 1982).

Discussion

Transport kinetics in the somatic oculomotor axons

The kinetics of cytoskeletal protein transport in somatic motor axons have been studied extensively in lumbar ventral motoneurons (Hoffman and Lasek, 1975; Hoffman et al., 1983; McQuarrie et al., 1986), hypoglossal motor neurons (Black, 1978; Heriot et al., 1985; and reviewed in Lasek, 1986), and phrenic motor neurons (Black, 1978). In particular, the studies on rat ventral motor neurons provide a basis for comparison with the kinetics of the somatic oculomotor axons.

The conventional approach for studying the kinetics of slow axonal transport is to analyze the passage of pulse-labeled proteins through one or more nerve segments. This approach can be applied directly to the somatic oculomotor axons of segment M1: because this segment contains only the somatic motor axons and these axons course uninterrupted through the segment, transport curves from segment M1 are directly related to the rate of transport through the somatic oculomotor axons.

The overall kinetics of slow transport in the somatic oculomotor axons are similar to those in rat ventral motor axons. In both types of axons, SCa and SCb occur as 2 distinct waves and SCa contains more radioactivity than does SCb (Fig. 2). The SCb and SCa peaks arrive at segment M1 at 2 and 7 d. This indicates that the transport rates of SCb and SCa in the somatic oculomotor axons are 5.5 and 1.6 mm/d, respectively. In rat ventral motor axons, the rates of SCb and SCa are 3.1 and 1.3 mm/d, respectively (McQuarrie et al., 1986). Next, we compare the detailed kinetics of individual cytoskeletal proteins in the somatic oculomotor and rat ventral motor axons.

SCb proteins

Like the ventral motor axons, somatic oculomotor axons have proteins that specifically identify the SCb wave. The 35 kDa protein is one of these SCb marker proteins (Fig. 5 and McQuarrie et al., 1986). In the somatic oculomotor axons, the 35 kDa protein is transported almost exclusively with the main SCb wave and has only a small trailing component that overlaps the neurofilaments in SCa. In contrast, the 125 kDa protein has a relatively large trailing component that lags behind the main SCb peak.

Garner and Lasek (1982) have proposed that the size of the trailing component for any SCb protein is a function of the affinity of the protein for the SCb "carrier complex" (reviewed by Lasek et al., 1984). In their model of slow axonal transport, proteins that have a small trailing component are tightly bound to the SCb carrier complex. According to this model and the shapes of the transport waves of segment M1, the 35 kDa protein apparently has a higher affinity for the carrier complex than does the 125 kDa protein.

Actin

In the somatic oculomotor axons, more actin is transported in SCa than in SCb. In segment M1, 13% of the actin traverses the somatic motor axons between 1 and 4 d, with the SCb wave, and 87% traverses the segment between 4 and 52 d, with the SCa wave. Likewise, in rat ventral motor axons, the amount of radioactive actin transported with the SCa wave exceeds that carried in the SCb wave (McQuarrie et al., 1986).

In contrast with the actin transport kinetics in oculomotor and ventral motor axons, most of the actin in retinal ganglion cell axons is transported with SCb, and only a small trailing component overlaps the SCa wave (Black and Lasek, 1980; Garner and Lasek, 1982; McQuarrie et al., 1986). McQuarrie et al. (1986) have proposed that the amount of actin transported in SCb and SCa is directly related to the number of microfilaments transported in these subcomponents of slow transport. On the basis of these observations, more microfilaments appear to be transported with SCa in motor axons than in retinal ganglion axons.

Tubulin

The transport curve of tublin in the somatic oculomotor axons is very similar to that in the ventral motor axons. In both cases, most of the tubulin is transported in SCa and a smaller amount in SCb. These kinetics have led to the proposal that these axons contain 2 types of microtubules (Lasek et al., 1983). This is supported by the observation that the tubulin isoforms in SCa differ from those in SCb (Tashiro and Komiya, 1983; Tashiro et al., 1984).

Detailed analyses of the SCa tubulin wave and the neurofilament wave in mammalian motor and sensory axons demonstrate that the peak of the SCa tubulin wave moves slightly faster than that of the neurofilament wave (McQuarrie et al., 1986). Likewise, in the chicken somatic oculomotor axons, the tubulin peak traverses segment M1 at 7 d and the neurofilament protein peak follows at 15 d (Fig. 6). These observations indicate that the mechanisms that coordinate the movements of the microtubules and neurofilaments permit the neurofilaments to lag behind the microtubules in these axons.

Neurofilament proteins

In ventral motor neurons, hypoglossal neurons, and phrenic motor neurons the neurofilament waves are bell-shaped, fairly symmetrical, and have a very small trailing component (Hoffman and Lasek, 1975; Black, 1978; Lasek, 1982; McQuarrie et al., 1986). This observation has led to the proposal that lateral interactions among the cytoskeletal polymers in the axon tend to coordinate the movements of the neurofilaments through the axon (Hoffman and Lasek, 1975; Black and Lasek, 1980; Lasek, 1981).

In the somatic oculomotor axons, the neurofilament wave has a main component that resembles the waveform of the neurofilament proteins in ventral motor axons. However, the wave is asymmetric in the somatic oculomotor axons and has a distinct trailing component. This indicates that in the somatic oculomotor axons, some of the neurofilaments move more slowly than those in the main wave.

The diversity of rates of neurofilament transport in the somatic oculomotor axons may be due in part to heterogeneity in the population of axons (Hoffman et al., 1983)—some of the somatic motor axons may have a slower rate of transport than others. An additional possibility is that the trailing neurofilament proteins represent a slowly moving population of neurofilaments that lags behind the main population in all of the somatic oculomotor axons (Hoffman et al., 1983; Nixon and Longvinenko, 1986).

Although these somatic oculomotor axons contain a slowly moving population of neurofilaments, Figure 6 shows that, at 83 d after injection, the radioactivity in segment M1 has reached background levels. This observation indicates that few, if any,

of the neurofilaments are stationary in somatic oculomotor axons, and confirms the results from studies on many other kinds of neurons (Hoffman and Lasek, 1975; Black, 1978; Mori et al., 1979; Black and Lasek, 1980).

Computer modeling the transport profiles of the parasympathetic axons

Like segment M1, segment G contains only a single population of axons, the parasympathetics. Unlike segment M1, segment G also contains axon terminals. In the terminals, specialized mechanisms remove the cytoskeletal proteins from the axons, and the rate at which these mechanisms operate affects the shape and amplitude of the transport curve in segment G. To obtain "pure" transport kinetics for the parasympathetic axons that are separate from the kinetics in the terminal regions, a new method of analysis was required. We will describe this method and then show how it can be used to separate the effects of the mechanisms in the terminal regions from the "pure" transport kinetics that characterize the proximal regions of the axon.

The pulse-transient: a mathematical summary of the transport profile

The shape and amplitude of each transport curve can be usefully summarized by the pulse-transient, which is obtained by integrating the total area under each transport curve. For the axons in any nerve segment, the pulse-transient is determined by (1) the length of the segment, (2) the total amount of radioactivity in the pulse-labeled wave, and (3) the rates at which the pulse-labeled wave enters, traverses, and exits the segment.

The pulse-transient in the parasympathetic axons of the oculomotor nerve. If segment length is held constant, the pulse-transient is relatively constant when sampled at different points along those regions of the axon that are proximal to the terminal region. For example, studies of motor axons in peripheral nerves demonstrate that the amount of radioactivity in the pulse-labeled slow transport wave remains relatively constant over distances of centimeters (Hoffman and Lasek, 1975; Lasek and Black, 1977; Black, 1978). On the basis of this observation, it is reasonable to extend these results to the oculomotor nerve and to assume that the pulse-transient of the proximal somatic motor axons (segment O2) is the same as that in the more distal motor divisions of the same nerve (segments M1 and M2).

All of the somatic motor axons in segment O2 are distributed to segments M1 and M2. In keeping with the above observations, the sum of the pulse-transients of segments M1 and M2 should be equal to OM, the pulse-transient of the somatic oculomotor axons in segment O2 of the oculomotor nerve (Table 1). Furthermore, by subtracting OM from the pulse-transient of segment O2, we obtain P, the pulse-transient of the parasympathetic axons in the oculomotor nerve.

The pulse-transient is greater in the axon terminals than in the axon proper. Table 1 compares P, the pulse-transient of the parasympathetic axons in the oculomotor nerve, with G, the pulse-transient of the terminal regions of these axons in the ciliary ganglion. In all cases, G was greater than P. For the total of slowly transported proteins, the ratio of G to P was 4.9; for individual proteins, the G/P ratio ranged from 3.9 for NF155 to 9.2 for tubulin. The segment sizes of G and P were held essentially constant (see legend Table 1); therefore, the increase in the pulse transients of G indicates that the transit rate through the axon terminal region in the ganglion is less than that through the axon proper in the oculomotor nerve. In other words, the slowly transported proteins spend more time in the axon terminal region than in equivalent lengths of the axon proper.

An algorithm that models mechanism in the terminals

The pulse-transient characterizes the total radioactivity in a transport curve. Another way to characterize transport curves is to describe their shapes in detail. To examine the effects of the axon terminals on curve shape, we devised an algorithm that models the transport curves as a function of the probability that a protein molecule will be removed from the axon terminals in 1 d:

$$R_t = R_{t-1} + A_t - FR_{t-1}$$

where R_t is the amount of radioactivity present in a terminal segment on day t, A is the amount of radioactivity transported into the terminal in a 1 d period, and F is the probability that a unit of radioactivity will be removed in 1 d.

One advantage of this algorithm is that, via computer, we can remove the changes in curve shape that are generated by mechanisms peculiar to the terminal regions of segment G. In this way, we obtain "pure" transport curves that are characteristic of the proximal regions of the parasympathetic axons; in essence, we can view the transport curves as if the axons in segment G continued uninterrupted through G, without terminating. These "pure" curves of parasympathetic axons can then be directly compared with the transport curves of the somatic motor axons of segment M1, where there are no terminals.

Computer-modeling experiments

Radiolabeled cytoskeletal proteins enter the axon terminals by slow axonal transport and are finally removed by proteolytic degradation. In the model, we assume that axonally transported proteins are removed from the terminal by mechanisms that can be approximated as a simple, first-order stochastic process (Lajtha and Marks, 1971). Specifically, every molecule of a particular class of protein (e.g., tubulin) has an equal and independent probability of being removed during its residence in the axon terminal. For the sake of simplicity, the algorithm operates in discrete 1 d steps; thus, the total amount of radiolabeled protein in a terminal today equals (1) the labeled protein that was in the terminal yesterday, *plus* (2) the labeled protein added since yesterday via axonal transport, *minus* (3) the labeled protein lost by a simple stochastic process. (This simple stochastic process depends on the probability that any individual protein will be removed in 1 d, and, using the standard equation for calculating the removal of units by a stochastic process—$N_t = N_0e^{-kt}$—we have expressed the probability as the half-residence time of a protein in a terminal.)

Modeling neurofilament protein transport. The transport curve of the neurofilament proteins in segment M1 is an example of a typical pulse-labeled wave on its way to the terminals (Fig. 7). What happens to the shape of the curve when the pulse-labeled wave enters the terminal region? This depends on the operation of protein-removal mechanisms in the terminals, as reflected by the half-residence time of the proteins. In a typical simulation, the pulse-labeled wave enters a hypothetical segment MG that is located 11 mm from the brain stem. Segment MG contains the terminals of the somatic motor axons; Figure 7 shows how the transport curve in hypothetical segment MG changes if the half-residence time is increased from 0 to more than 100 d.

At one extreme, when the half-residence time of the proteins

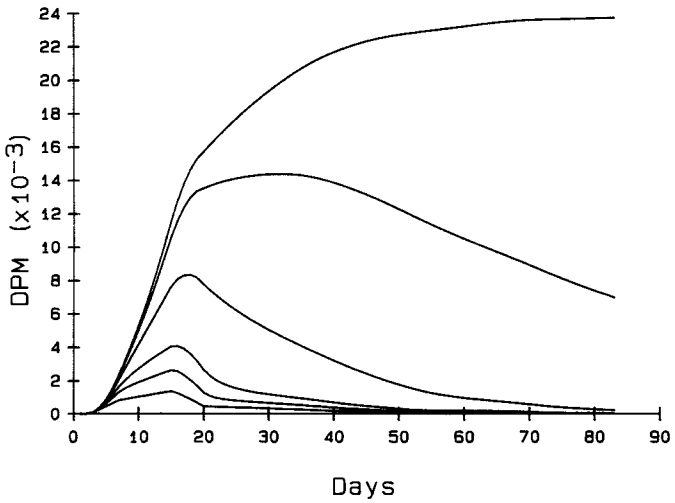

Figure 7. Computer experiments modeling the effects of the half-residence time on the shape and amplitude of pulse-labeled neurofilament proteins in the somatic motor axons. In the computer experiments, the pulse-labeled wave from segment M1 (Fig. 6) is transported into a hypothetical segment MG located 11 mm from the oculomotor nucleus. Segment MG contains the axon terminals of the somatic motor axons, and the residence of the neurofilament proteins in the terminals is varied from 0 to 1, 2, 7, 27, and >100 d consecutively, reading from *bottom to top.* For details see the text.

in the axon terminals of segment MG is 0, the shape of the MG transport curve is the same as that of M1 (compare Figs. 5 and 7); here, the axon terminals have no affect on the shape of the transport curve. In contrast, if the half-residence time is increased to 1 or 2 d, the amplitude of the MG wave increases. Additional increases of the half-residence time continue to change the shape of the curve dramatically—specifically, the slope of the initial ascending part of the wave increases, and the wave broadens substantially.

Although the shape of the curve changes in response to increases in the half-residence time, the initial intercept of the transport curve remains unaffected (Fig. 7). The initial intercept corresponds to the time when the first radiolabeled proteins arrive at a segment, and provides a precise way to measure the maximal rate of axonal transport. This measurement is independent of the removal processes in the axon terminals. For instance, using the initial intercepts of the neurofilament curves in Figure 5, we estimate that the maximal rates of neurofilament transport are 3.2 mm/d for somatic motor axons and 1.6 mm/d for parasympathetic axons (Table 2).

Modeling "pure" transport curves for the parasympathetic axons. What is the shape of transport curves for the parasympathetic axons alone? In the chicken oculomotor system, we could not easily measure these "pure" transport curves directly; thus, we used our algorithm to infer these curves from actual ciliary ganglion data, the transport curves of segment G. With the algorithm, we adjusted the radioactivity curves of the segment G curves by varying the half-residence time of the proteins in the terminals; basically, we attempted to undo the effects of the normal removal processes in the ganglia.

Specifically, the half-residence time was varied with a computer, and a number of simulated waves were generated. For each wave, the pulse-transient was obtained by integrating the area under the computer-generated curve. If the terminals were not present in segment G, the pulse-transient would remain approximately constant as the pulse-labeled wave passed through the axons. Thus, we searched for a computer-generated curve with a pulse-transient matching the known pulse-transient of the parasympathetic axons (as inferred from the data of Table 1).

Table 1. Pulse-transients for total slowly transported proteins and for individual SCa and SCb proteins in segments of the oculomotor system

Proteins	O2	OM (M1 + M2)	G	P (O2–OM)	G/P
Total proteins	16,080	10,964	24,908	5116	4.9
Actin	2915	1958	5466	957	5.7
Beta-tubulin	6552	5570	9015	926	9.2
NF155	8139	6900	4800	1239	3.9
Brain spectrin	1469	1264	1530	205	7.5
110 kDa	2272	1774	4208	498	8.5
60 kDa	2232	1670	3370	562	6.0
35 kDa	3199	2151	6419	1048	6.1

The pulse-transients are reported as dpm × 10^{-2} for 1.5 mm of oculomotor nerve (O2) and its somatic motor branches (OM = M1 + M2), and one ganglion (G). To correct for the difference between the segment length of G, which was 1 mm long, and that of the other segments, all of the results were normalized to a segment length of 1.5 mm.

Figure 8 shows the results of these computer simulations of "pure" transport curves for the 35 kDa protein, actin, tubulin, and the neurofilament proteins in the parasympathetic axons. In Figure 8, these curves are compared with the actual transport curves of the ciliary ganglion from which they were generated, and the transport curves of the somatic motor axons.

Transport kinetics in the parasympathetic axons

Table 2 compares the transport rates in somatic motor axons with those in parasympathetic axons, which were obtained by the computer simulation. The rates of SCb, which were determined from the arrival times of the 35 kDa protein, were similar in these axons. By contrast, the rates of SCa, which were de-

Table 2. Rate of transport SCa and SCb proteins in somatic motor (M) and parasympathetic (P) axons

	Arrival rate (mm/d)		Main wave rate (mm/d)	
Proteins	M	P	M	P
SCb				
35 kDa	11	11	1.6–5.5 (2–7 d)	1.6–5.5 (2–7 d)
Actin	11	11	0.5–5.5 (2–20 d)	0.5–5.5 (2–20 d)
Tubulin	11	11	0.5–1.6 (7–20 d)	1.6–5.5 (2–7 d)
SCa				
NFP	3.2	1.6	0.5–2.2 (5–20 d)	0.22–1.1 (10–50 d)

Arrival rates were estimated using fluorographs of segment M1 (somatic motor axons) or segment G (parasympathetic axons) to determine when the proteins first arrived at these segments, which are both 11 mm from the oculomotor nucleus. Main wave rates were estimated from the time (shown in parentheses) required for the main portion of the transport waves shown in Figure 8 to traverse the somatic motor and parasympathetic axons. Note that the estimates for the main wave transport rates of the parasympathetic axons were obtained from the computer-simulated "pure" transport waves.

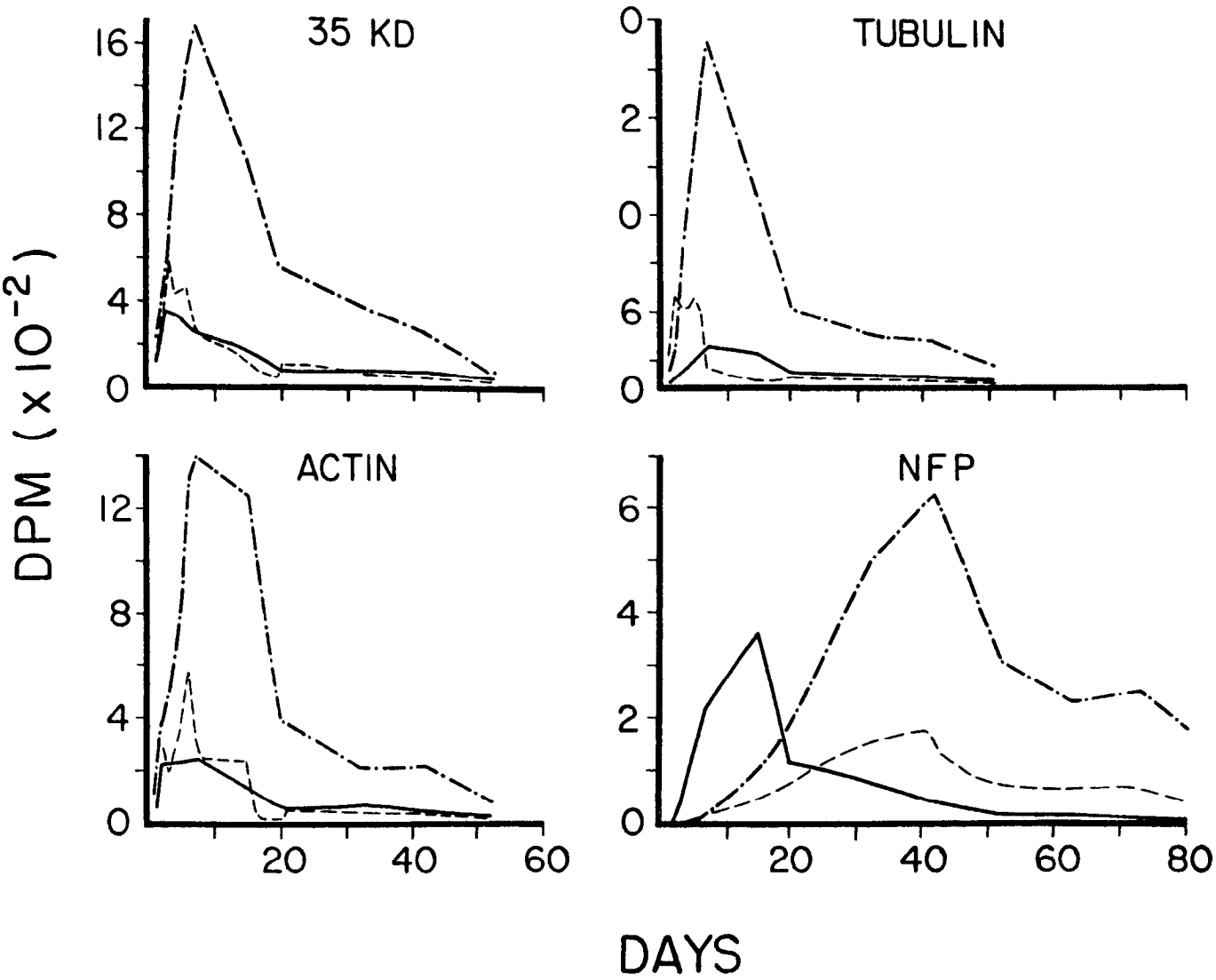

Figure 8. Computer-simulated "pure" transport profiles for the parasympathetic axons (*dashed lines*) are compared with profiles from the terminal regions in the ciliary ganglion (*dots and dashes*) and with profiles from the somatic motor axons (*solid lines*). The computer model simulates "pure" transport curves from the radiolabeling profiles of the ciliary ganglion. In the computer model, the half-residence time of the proteins in the terminal regions is used to remove the radioactivity that was added to the ciliary ganglion during the residence of the radiolabeled proteins in the terminal regions (see the text for details). To effectively compare the computer-simulated transport profiles of the parasympathetic with those of the somatic motor axons, the waveform of the somatic motor axons was normalized relative to that of the parasympathetic axons. Waveforms were normalized using the pulse-transient—the total integrated area under the waveforms—by the following formula: (Pulse-transient of parasympathetic/pulse-transient of somatic motor) × each value for the somatic motor axons.

termined by the arrival times of the neurofilament proteins, differed. Next, we compared the detailed patterns of the computer-simulated "pure" transport curves of the parasympathetic axons with the actual transport curves of the somatic oculomotor axons (Fig. 8).

The 35 kDa protein and other SCb proteins

The overall shape of the computer-simulated transport curve for the 35 kDa protein was similar to that of the actual curve for the somatic motor axons (Fig. 8). In both cases, the transport curve had a main wave that traversed the axons between 2 and 7 d, or at a rate of 1.5–5.5 mm/d, and both had a trailing component between 7 and 20 d. Because the 35 kDa protein is one of the chief components of SCb, these results indicate that the rate of SCb is similar for the somatic motor and parasympathetic axons (Table 2).

Actin

The overall shape of the computer-simulated "pure" transport curve of actin in the parasympathetic axons was also the same as the actin transport curve in the somatic motor axons (Fig. 8). In both cases, the curves had an initial front that reached a peak at 2 d, and this front coincided with the SCb wave front. The initial front was followed by a broad wave that traversed the axons between 2 and approximately 20 d. These results indicate that actin traverses the somatic motor and parasympathetic axons at approximately the same rate, 0.5–5.5 mm/d (Table 2).

Although the overall shape of the distribution of the computer-simulated actin curve of the parasympathetic axons overlapped the actin transport curve of the somatic motor axons, the detailed shapes differed. Specifically, the computer-simulated curve had a large sharp peak at 6 d, while the actual somatic

motor curve had a much smaller peak at 7 d. In addition, the computer-simulated curve declined abruptly at 17 d, but the actual somatic motor curve declined gradually during this period. These detailed aspects of the computer-simulated curve must be interpreted cautiously. The algorithm magnifies changes in slope of the actual transport curve, and the curve for the ciliary ganglion is constructed from a relatively small number of points connected by straight lines. Thus, the transport curves for the ciliary ganglion are not as smooth as they would be if all the data points were available, and the computer model exaggerates the detailed features of the segment G curve.

Tubulin

The computer-simulated "pure" transport curve for tubulin in the parasympathetic axons clearly differed from that of the somatic motor axons (Fig. 8). For the parasympathetic axons, the computer-simulated curve suggests that the main wave of tubulin traversed the region between 2 and 7 d (1.6–5.5 mm/d); here, tubulin corresponds very closely to the SCb wave, as exemplified by the 35 kDa protein (Table 2). Notably, very little of the transported tubulin overlaps the wave of transported neurofilament proteins in the parasympathetic axons, and it appears that the microtubules in the parasympathetic axons are transported to a great extent with the SCb proteins (Fig. 8; Table 2). In contrast, in many other axons (including the somatic oculomotor axons), a large fraction of the transported tubulin moves in coordination with the neurofilaments in SCa (Hoffman and Lasek, 1975; Black and Lasek, 1980; McQuarrie et al., 1986; Oblinger et al., 1987). The relative amount of tubulin that is transported with the neurofilaments in SCa and SCb may be a function of the organization of the axonal cytoskeleton and of the relationship between the microtubules and neurofilaments (Lasek, 1986; McQuarrie et al., 1986).

Neurofilament proteins

The overall shape of the simulated transport curve for the neurofilament proteins in the parasympathetic axons was like that of the somatic oculomotor axons (Fig. 8). The wave was asymmetric and consisted of 2 components—a main wave and trailing tail. Though the shapes of the waves were very similar, the rate of the neurofilament wave was much slower in the parasympathetic axons than in the somatic motor axons. The main peak arrived at 15 d (0.73 mm/d) in the somatic motor axons, and it arrived at 40 d (0.27 mm/d) in the parasympathetic axons. These results and the difference between initial intercepts of the transport curves indicate that the rate of neurofilament transport is 2–3 times faster in the somatic motor axons than in the parasympathetic axons (Table 2).

Electron-microscopic analyses of the cytoskeleton in the oculomotor axons suggest that the differences in the neurofilament transport rates may be related to differences in the packing density of the neurofilaments in these axons. The neurofilaments in the parasympathetic axons are 1.5 times more densely packed than in the somatic axons (Price et al., 1986). This tight packing of the neurofilaments in the parasympathetic axons may generate resistance and retard their transport in the axon.

Kinetics in the parasympathetic axon terminals: the half-residence time

In the computer simulation, the half-residence time was varied until the pulse-transient of the simulated transport curve matched the pulse-transient of the actual pulse-labeled wave in the oculomotor nerve; this provided an estimate of the half-residence time of the proteins in the ciliary ganglion.

From the computer-modeling experiments, the half-residence times are 2 d for the neurofilament proteins, 3.5 d for both actin and the 35 kDa protein, and 7 d for tubulin. These half-residence times are determined from the time needed for the removal of radiolabeled proteins from the axon terminal region, and they are the inverse function of the rate at which the proteins are removed from the terminals. Thus, our results indicate that the neurofilaments are removed most rapidly from the terminal regions and that tubulin is removed most slowly. Next we discuss the mechanisms that contribute to the half-residence times of the cytoskeletal proteins in the terminal regions of the parasympathetic axons.

The 35 kDa protein and other SCb proteins

The half-residence times of the SCb proteins range from 3.5 d for the 35 and 60 kDa proteins to 5 d for the 110 kDa protein, which suggests that these proteins are removed rather slowly from the terminals. The rate of removal critically determines the amount of cytoskeletal proteins in the terminals (Lasek and Katz, 1987); the number of proteins in the terminal is inversely proportional to their rate of removal. On this basis, we expect that the number of SCb proteins in the terminals is greater than that in the axon proper. This prediction is supported by immunocytochemical studies that show that SCb proteins, such as calmodulin, clathrin, and brain spectrin, are more abundant in the terminal than in the proxmal region of the axon (De Lorenzo, 1982; Puszkin et al., 1983; Walker et al., 1985).

Actin

Like some of the SCb proteins, the half-residence time of actin is 3.5 d; and actin is more abundant in the axon terminal than in the axon proper. The milieu in the terminal bouton favors the polymerization of microfilaments, and microfilaments are the principal structural elements of the terminal cytoskeleton (Blitz and Fine, 1974; Black, 1978; Black and Lasek, 1980; Drenckhahn and Kaiser, 1983; Walker et al., 1985). Apparently, a significant fraction of the actin in the terminals is sequestered in microfilaments and this may contribute to the longevity of the actin in the terminals.

Tubulin

Tubulin has the longest half-residence time of the cytoskeletal proteins in the ciliary ganglion. In the axon, tubulin is transported in microtubules; nonetheless, microtubules do not accumulate in the axon terminals (Peters et al., 1976). The microtubles appear to depolymerize in the terminals, and the tubulin that is released is apparently added to the pool of monomeric tubulin in the terminal bouton (Brady, 1981; Schliwa et al., 1981; Black et al., 1984; Brady et al., 1984). Our observation that tubulin has a half-residence time of 7 d suggests that the monomeric tubulin is degraded very slowly after it is released from the microtubules in the terminals.

Neurofilament proteins

The neurofilament proteins have the shortest half-residence time (2 d) of the cytoskeletal proteins. Though these proteins are removed more quickly from the terminal regions than other cytoskeletal proteins, half the neurofilament proteins that enter the terminal region reside there, on average, 2 d longer than they reside in the axon proper. On the basis of this observation,

we expect that the axon terminal regions in the ciliary ganglion contain more neurofilaments than the axons in an equally long segment of oculomotor nerve.

Electron-microscopic studies of the ciliary ganglion (Cantino and Mugnaini, 1975; and unpublished observations) show that the terminal boutons of the parasympathetic axons have few, if any, neurofilaments. Apparently, the neurofilaments are rapidly disassembled when they enter the terminal boutons. Neurofilaments are extemely stable polymers, and the disassembling of these structures requires the action of specific proteases that normally operate only in the specialized milieu of the terminal bouton (Lasek and Hoffman, 1976; Roots, 1983).

In contrast with the paucity of neurofilaments in the terminal boutons, numerous neurofilaments are present in the preterminal axons in the ciliary ganglion. Furthermore, the preterminal axons branch extensively (Lenhossek, 1911; Terzuolo, 1951) and it may take longer for the slow transport mechanisms to move the neurofilaments through these tortuous branches than it does to move them through the straight segments of the parasympathetic axons in the oculomotor nerve. A slow transit rate for neurofilaments through the preterminal branches will delay their entry into the terminal boutons and postpone their degradation by the terminal proteases. Thus, the tortuous preterminal branching pattern of the parasympathetic axons may contribute to the residence time of the neurofilaments in the ciliary ganglion.

Conclusion: the removal mechanisms control the composition of the cytoskeleton in the axon terminal

Our kinetic studies of pulse-labeled proteins in oculomotor axons indicate that, in the terminal region, the residence times of cytoskeletal proteins differ. Neurofilament proteins have the shortest half-residence time (2 d), which confirms the proposal that these proteins are rapidly eliminated when the neurofilaments are transported into the terminal boutons (Lasek and Hoffman, 1976; Black and Lasek, 1980; Roots, 1983). In contrast to the neurofilament proteins, actin and tubulin have half-residence times of 3.5 and 7 d, respectively. These differences in the residence times of the cytoskeletal proteins of the axon terminals indicate that the proteins are removed from the terminals at different rates. By controlling the residence times of the cytoskeletal proteins in the terminals, the degradative mechanisms that remove the proteins from the terminals critically determine the relative amount of each of these proteins in the axon terminal; they control the composition of the cytoskeleton in the axon terminal. Through their effects on the composition of the cytoskeleton after it is transported from the axon proper into the terminal, these mechanisms are an important part of the system that converts the cytoskeleton of the axon proper into the specialized cytoskeleton of the axon terminal.

References

Bennett, G., L. Di Giamberardino, H. L. Koenig, and B. Droz (1973) Axonal migration of protein and glycoprotein to nerve endings. II. Radioautographic analysis of the renewal of glycoproteins in nerve endings of chicken ciliary ganglion after intracerebral injection of (3H) fucose and (3H) glucosamine. Brain Res. *60:* 129–146.

Black, M. M. (1978) Axonal transport of cytoskeletal proteins. Ph.D. thesis, Case Western Reserve University.

Black, M. M., and R. J. Lasek (1979) Axonal transport of actin: Slow component b is the principal source of actin for axon. Brain Res. *171:* 401–413.

Black, M. M., and R. J. Lasek (1980) Slow components of the axonal transport: Two cytoskeletal networks. J. Cell Biol. *86:* 616–623.

Black, M. M., J. M. Cochran, and J. T. Kurdyla (1984) Solubility properties of neuronal tubulin: Evidence for labile and stable microtubules. Brain Res. *295:* 255–263.

Blitz, A. L., and R. E. Fine (1974) Muscle-like contractile proteins and tubulin in synaptosomes. Proc. Natl. Acad. Sci. USA *71:* 4472–4476.

Bonner, W. M., and R. A. Laskey (1984) A film detection method for tritium labelled proteins and nucleic acids in polyacrylamide gels. Eur. J. Biochem. *46:* 83–88.

Brady, S. T. (1981) Biochemical and solubility properties of axonal tubulin. J. Cell Biol. *91:* 333a.

Brady, S. T., and R. J. Lasek (1982) Axonal transport: A cell-biological method for studying proteins that associate with the cytoskeleton. Methods Cell Biol. *25:* 365–398.

Brady, S. T., M. Tytell, and R. J. Lasek (1984) Axonal tubulin and axonal microtubules: Biochemical evidence for cold stability. J. Cell Biol. *99:* 1716–1724.

Cantino, D., and E. Mugnaini (1975) The structural basis for electrotonic coupling in the avian ciliary ganglion. A study with thin sectioning and freeze-fracturing. J. Neurocytol. *4:* 505–536.

De Lorenzo, R. J. (1982) Calmodulin in neurotransmitter release and synaptic function. Fed. Proc. *41:* 2265–2272.

Di Giamberardino, L., G. Bennett, H. L. Koenig, and B. Droz (1973) Axonal migration of protein and glycoprotein to nerve endings. III. Cell fraction analysis of chicken ciliary ganglion after intracerebral injection of labeled precursors of proteins and glycoproteins. Brain Res. *60:* 147–159.

Drenckhahn, D., and H. W. Kaiser (1983) Evidence for the concentration of F-actin and myosin in synapses and in the plasmalemmal zone of axons. Eur. J. Cell Biol. *31:* 235–240.

Droz, B., H. L. Koenig, and L. Di Giamberardino (1973) Axonal migration of protein and glycoprotein to nerve endings. I. Radioautographic analysis of the renewal of protein in nerve endings of the chicken ciliary ganglion after intracerebral injection of 3H-lysine. Brain Res. *60:* 93–127.

Filliatreau, G., and L. Di Giamberardino (1982) Quantitative analysis of axonal transport of cytoskeletal proteins in chicken oculomotor nerve. J. Neurochem. *39:* 1033–1037.

Garner, J. A., and R. J. Lasek (1982) Cohesive axonal transport of the slow component b complex of polypeptides. J. Neurosci. *2:* 1824–1835.

Heriot, K., P. Gambetti, and R. J. Lasek (1985) Proteins transported in slow components a and b of axonal transport are distributed differently in the transverse plane of the axon. J. Cell Biol. *100:* 1167–1172.

Hoffman, P. N., and R. J. Lasek (1975) The slow component of axonal transport: Identification of major structural polypeptides of the axon and their generality among mammalian neurons. J. Cell Biol. *66:* 351–366.

Hoffman, P. N., R. J. Lasek, J. W. Griffin, and D. L. Price (1983) Slowing of the axonal transport of neurofilament proteins during development. J. Neurosci. *3:* 1694–1700.

Kamakura, K., S. Ishiura, H. Sugita, and Y. Toyokura (1983) Identification of Ca^{2+}-activated neutral protease in the peripheral nerve and its effects on neurofilament degeneration. J. Neurochem. *40:* 908–913.

Laemmli, V. K. (1970) Cleavage of structural proteins during the assembly of the head of bacteriophage T4. Nature *227:* 680–685.

Lajtha, A., and N. Marks (1971) Protein turnover. In *Handbook of Neurochemistry,* Vol. 5, pt. B, A. Lajtha, ed., p. 554, Plenum, New York, London.

Lasek, R. J. (1981) The dynamic ordering of neuronal cytoskeletons. Neurosci. Res. Prog. Bull. *19:* 7–32.

Lasek, R. J. (1982) Translocation of the neuronal cytoskeleton and axonal locomotion. Phil. Trans. R. Soc. Lond. [Biol.] *299:* 313–327.

Lasek, R. J. (1986) Polymer sliding in axons. J. Cell Sci. (Suppl.) *5:* 161–179.

Lasek, R. J., and M. M. Black (1977) How do axons stop growing? Some clues from the metabolism of the proteins in the slow component of axonal transport. In *Mechanisms, Regulation and Special Functions of Protein Synthesis in Brain,* S. Roberts et al., eds., pp. 161–169, Elsevier/North-Holland, New York.

Lasek, R. J., and S. T. Brady (1982) The structural hypothesis of axonal transport: Two classes of moving elements. In *Axoplasmic Transport,* D. G. Weiss, ed., pp. 397–405, Springer-Verlag, Berlin.

Lasek, R. J., and P. N. Hoffman (1976) The neuronal cytoskeleton, axonal transport and axonal growth. Cold Spring Harbor Conf. Cell Prolif. *3:* 1021–1049.

Lasek, R. J., and M. J. Katz (1987) Mechanisms at the axon tip regulate metabolic processes critical to axonal elongation. Prog. Brain Res. *71:* 49–60.

Lasek, R. J., I. G. McQuarrie, and S. T. Brady (1983) Transport of cytoskeletal and soluble proteins in neurons. In *Biological Structures and Coupled Flows,* A. Oplatka and M. Balaban, eds., pp. 329–347, Academic, New York/Balaban, Rehovot.

Lasek, R. J., J. A. Garner, and S. T. Brady (1984) Axonal transport of the cytoplasmic matrix. J. Cell Biol. *99:* 212s–221s.

Laskey, R. A., and A. D. Mills (1975) Quantitative film detection of 3H and 14C in polyacrylamide gels by fluorography. Eur. J. Biochem. *56:* 335–341.

Lenhossek, Von M. (1911) Das Ganglion ciliare der Vogel. Archiv Mikrosk. Anat. *76:* 745–769.

Levine, J. E., and M. B. Willard (1980) The composition and organization of axonally transported proteins in the retinal ganglion cells of the guinea pig. Brain Res. *194:* 137–154.

Malik, M. N., M. D. Fenko, and H. M. Wisniewski (1984) Purification and partial characterization of two forms of Ca^{2+}-activated neutral protease from calf brain synaptosomes and spinal cord. Neurochem. Res. *9:* 233–240.

McQuarrie, I. G., S. T. Brady, and R. J. Lasek (1986) Diversity in the axonal transport of structural proteins: Major differences between optic and spinal axons in the rat. J. Neurosci. *6:* 1593–1605.

Mori, H., M. Komiya, and M. Kurokawa (1979) Slowly migrating axonal polypeptides. Inequalities in their rate and amount of transport between two branches of bifurcating axons. J. Cell Biol. *82:* 174–184.

Nixon, R. A., and R. B. Longvinenko (1986) Multiple fates of newly synthesized neurofilament proteins: Evidence for a stationary neurofilament network distributed nonuniformly along the axons of retinal ganglion cell neurons. J. Cell Biol. *102:* 647–659.

Oblinger, M. M., S. T. Brady, I. G. McQuarrie, and R. J. Lasek (1987) Cytotypic differences in the protein composition of the axonally transported cytoskeleton in mammalian neurons. J. Neurosci. *7:* 453–462.

O'Farrel, P. H. (1975) High resolution two dimensional electrophoresis of proteins. J. Biol. Chem. *250:* 4007–4021.

Pant, H. C., and H. Gainer (1980) Properties of calcium-activated protease in squid axoplasm which selectively degrades neurofilament proteins. J. Neurobiol. *11:* 1–12.

Peters, S., S. L. Palay, and H. de F. Webster (1976) *The Fine Structure of the Nervous System: The Neurons and Supporting Cells,* pp. 124–130, W. B. Saunders, Philadelphia, PA.

Price, R. L., P. Paggi, and R. J. Lasek (1986) The density of neurofilaments differs in the somatic motor and parasympathetic oculomotor axons of chickens. In *Proceedings of the 44th Annual Meeting of the Electron Microscopy Society of America,* G. W. Bailey, ed., pp. 276–277, San Francisco Press, San Francisco, CA.

Puszkin, S., A. Andres, C. Ores, M. P. Lisanti, and W. J. Schook (1983) Immunocytochemical characterization of clathrin-associated proteins (CAPs). I. Neuronal distribution of CAPs, a component of clathrin-coated vesicles. Cell Tissue Res. *231:* 495–505.

Roots, B. I. (1983) Neurofilament accumulation induced in synapses by leupeptin. Science *221:* 971–972.

Schlaepfer, W. W., and S. Micko (1979) Calcium-dependent alterations of neurofilament proteins of rat peripheral nerve. J. Neurochem. *32:* 211–219.

Schlaepfer, W. W., and V. P. Zimmerman (1985) Calcium-activated proteolysis of intermediate filaments. In *Intermediate Filaments,* F. Wang et al., eds., Ann. NY Acad. Sci. *455:* 552–562.

Schliwa, M., U. Euteneuer, J. C. Bulinski, and J. Izant (1981) Calcium lability of cytoplasmic microtubules and its modulation by microtubule-associated proteins. Proc. Natl. Acad. Sci. USA *78:* 1037–1041.

Tashiro, T., and Y. Komiya (1983) Two distinct components of tubulin transport in sensory axons of the rat recognized by dimethylsulfoxide treatment. Biomed. Res. *4:* 443–450.

Tashiro, T., M. Kurokawa, and Y. Komiya (1984) Two populations of axonally transported tubulin differentiated by their interactions with neurofilaments. J. Neurochem. *43:* 1220–1225.

Terzuolo, C. A. (1951) Ricerche sul ganglio ciliare degli uccelli. Connessioni e mutamenti in relazione all 'eta' e dopo recisione delle fibre prepangliari. Z. Zellforsch. *36:* 255–267.

Tytell, M., M. M. Black, J. A. Garner, and R. J. Lasek (1981) Axonal transport: Each major rate component reflects the movement of distinct macromolecular complexes. Science *214:* 179–181.

Walker, J. H., C. H. Boustead, V. Veitzemann, G. Show, K. Weber, and M. Osborn (1985) Cytoskeletal proteins at the cholinergic synapse: Distribution of desmin, actin, fodrin, neurofilaments, and tubulin in *Torpedo* electric organ. Eur. J. Cell Biol. *38:* 123–133.